sciendo

Int. J. Appl. Math. Comput. Sci., 2025, Vol. 35, No. 3, 479–492
DOI: 10.61822/amcs-2025-0034

amcs

MODELING PROPAGATION OF WEAKLY ADVANTAGEOUS MUTATIONS IN CANCER CELLS

ANDRZEJ POLAŃSKI [a,*], MATEUSZ KANIA [b], JAROSŁAW GIL [a], WOJCIECH ŁABAJ [a], EWA LACH [a], AGNIESZKA SZCZĘSNA [a]

[a]Department of Computer Graphics, Vision and Digital Systems
Silesian University of Technology
Akademicka 16, 44-100 Gliwice, Poland
e-mail: andrzej.polanski@polsl.pl

[b]Department of Applied Informatics
Silesian University of Technology
Akademicka 16, 44-100 Gliwice, Poland

There is recent evidence that a considerable proportion of somatic mutations in cancer cells' DNA may exert a weakly advantageous effect on tumor growth. In this paper, we develop models of cancer evolution with somatic mutations that introduce a weakly advantageous force to the evolution of cancer cells. The elaborated models incorporate random events of cellular births, deaths and occurrences of somatic mutations in cancer cells' DNA. The models belong to two categories: deterministic and stochastic. The former are based on systems of differential equations that balance the average number of cells and mutations during evolution. To verify the results of our deterministic modeling, we use a stochastic Gillespie algorithm. We show that our models predict the explosive growth of the cancer cells population, consistent with recent experimental observations.

Keywords: cancer evolution, Gillespie algorithm, mutation wave modeling.

1. Introduction

The growth of cancer cellular population is a highly variable and complex process with several genomic and physiological components. Many important properties and parameters of this process remain disputable, and much research is necessary for better understanding how tumors change during growth and under therapy (Greaves and Maley, 2012). Developing and studying mathematical models of cancer evolution and confronting their outcomes with experimental data can help discovering roles and estimating strengths of various factors behind cancer onset and progression.

A long-standing area of research in cancer modelling is fitting various mathematical models to temporal, experimental data on tumour growth (e.g., Laird, 1964; Brú *et al*., 2003; West and Newton, 2019; Talkington and Durrett, 2015; Vaghi *et al*., 2020; Kühleitner *et al*., 2019). Scenarios in the cited researches included exponential growth models, power law models with exponent lower then one leading to growth slowing down in time, Von Bertalanffy and Kleiber, saturating growth models, Gompertzian, logistic, etc. A variety of growth scenarios and divergent conclusions regarding growth types, exponential, slowing down or saturating, result from the inherent difficulty in inferring growth type from temporal data over rather short periods of time.

The recent advancements of experimental techniques for monitoring neoplastic transformations have facilitated the acquisition of novel insights for the study of tumour growth. The application of PET (positron emission tomography) techniques enables the estimation of tumour growth rates, as determined by the intensity of glucose intake (Pérez-García *et al*., 2020). The results published by Pérez-García *et al*. (2020) yielded a groundbreaking conclusion: the growth of several cancers follows a superlinear power law, i.e., a power law model with an exponent greater than one. This

*Corresponding author

© 2025 A. Polański et al.
This is an open access article distributed under
the Creative Commons Attribution-NonCommercial-NoDerivs license
(http://creativecommons.org/licenses/by-nc-nd/4.0/).

conclusion leads to scenarios of tumor growth of explosive type, with finite escape times. It thus calls for research into the explanations (physiological, metabolic, genetic/genomic, geometric/spatial) of such scenarios. Models of explosive tumor growth have already appeared in the literature (Pérez-García *et al*., 2020; Azimzade *et al*., 2021; Bosque *et al*., 2023). These studies used versions of Fisher–Kolmogorov (FK) partial differential equations as a mathematical background, however their constructions were based of different views and principles. Pérez-García *et al*. (2020) proposed the model of the form of three dimensional FK equation with cell diffusion and two types (size-independent and size-dependent) cellular proliferation processes taking place in the environment/medium of a given capacity. Bosque *et al*. (2023) introduced the model incorporating cell migration, proliferation with phenotypic transitions and interference between clones with different phenotypes competing for the available space. Again, it was assumed that tumor growth occurs in the environment of a given capacity. Finally, Azimzade *et al*. (2021) developed a more complex and detailed model, of the form of a system of FK equations, with fitness advantages of cancer cells caused by driver mutations, dynamics of cellular oxygen consumption and angiogenesis.

The present paper develops a mathematical model of tumour growth driven by the propagation of weakly advantageous somatic mutations in cancer cells. Somatic mutations in cancer cells are usually classified as either drivers or passengers (e.g., Greaves and Maley, 2012). Driver mutations are rare but have a strong causal effect on cancer development, while passenger mutations are abundant in cancer cells DNA but have little or no effect on cancer development. Searching for driver mutations in cancer DNA and researching their roles in cancer growth plays a crucial role in understanding processes underlying oncogenesis (e.g., ICGC/TCGA PCWG Consortium, 2020; Vogelstein and Kinzler, 2015). The number of driver mutations discovered/detected in a cancer cell population (in a sample from a cancer patient) is typically very low. These few drivers (Vogelstein and Kinzler, 2015) are always accompanied by large numbers of somatic passenger mutations. In contrast to driver mutations, impact of these numerous passenger mutations on cancer onset and/or development is actually rather not well understood (Kumar *et al*., 2020). Due to its high significance the issue of the role of passenger mutations in cancer has been studied by using/combining experimental/clinical observations, repositories of cancer DNA sequencing data (ICGC/TCGA PCWG Consortium, 2020; Cerami *et al*., 2012; WSI, 2022), tools of comparative genomics (Fu *et al*., 2014), statistics and mathematical modeling (Bozic *et al*., 2010; Kumar *et al*., 2020; McFarland *et al*., 2013).

One viewpoint in the literature on cancer genomics is that all passenger mutations are fully neutral and have no effect on tumour progression/evolution. This opinion was presented in several studies (Bozic *et al*., 2010; Williams *et al*., 2016; Tung and Durrett, 2021) supported by analyses of data from the ICGC/TCGA next-generation sequencing project (Wilks *et al*., 2014). The rationale for the full neutrality hypothesis provided by Bozic *et al*. (2010) was based on the consistency of predictions of the branching process model of cancer growth with allelic frequencies of driver and passenger mutations seen in sequencing data. Williams *et al*. (2016) introduced a mathematical model for variant allele frequencies (VAF) in an exponentially growing population, which predicted the 1/f power law of distribution of VAFs of fully neutral passenger mutations, quite consistent with observational data of next-generation sequencing of cancer tissues. Some authors (McDonald *et al*., 2018; Noorbakhsh and Chuang, 2017; Wang *et al*., 2018) pointed out that VAF statistics following from the model of Williams *et al*. (2016) can also be reproduced by other models, with not necessarily fully neutral mutations. Tung and Durrett (2021) used the multi-type branching processes model for studying the possibility of distinguishing neutral from advantageous mutations.

Recently, many researches have been bringing arguments that accumulated passenger mutations can impact cancer evolution, parallel/addition to drivers. Several authors observed that statistics (patterns of allelic frequencies) of passenger mutations differ between different cancers. Mc Farland *et al.* (2013; 2014) analyzed somatic mutations available in the Cosmic database (WSI, 2022) and, by studying their potential molecular impact using the bioinformatic tool PolyPhen (Boyko *et al*., 2008), hypothesized that majority of the passenger mutations are likely to exert a mildly damaging effect on the evolution of cancer cells population. Following this hypothesis, they have developed a mathematical model of cancer evolution with two counteracting factors, frequent passenger mutations, each with a weak deleterious effect and rare, driver mutations. Accumulated passenger mutations caused a slow shrinking of the cancer population, while rare driver mutations introduced selective sweeps, i.e., short time intervals of rapid population growth. Jiao *et al*. (2020) and Salvadores *et al*. (2019) demonstrated that genomic locations and frequencies of somatic mutations can be used to construct molecular signatures to distinguish between cancer types and their progression scenarios. In the recent research, Kumar *et al*. (2020) used quantitative molecular functional impact score (Fu *et al*., 2014) and evolutionary conservation measure (Davydov *et al*., 2010) to quantify the cumulative fitness effects of passenger mutations on tumour growth. Applying these scores to data on pan-cancer whole genome sequencing (ICGC/TCGA PCWG Consortium, 2020), they concluded

that aggregated effect of passengers plays a role in tumorigenesis beyond standard drivers and may either introduce a weakly deleterious impact or may generate a mildly driving (advantageous) evolutionary force.

As outlined above there is an experimental evidence on the occurrence of weakly advantageous somatic mutations in cancer cells. Therefore, we elaborate and analyze mathematical and computational models of oncogenesis driven by weakly advantageous mutations. Our approach is inspired by the model published by McFarland *et al*. (2013). We simplify it by including only one type of mutations, weakly advantageous. We also modify the relation for the cell deaths process, compared to the results of McFarland *et al*. (2013), by assuming that cell deaths occur with the intensity given by the power function with exponent parameter A. Allowing different values of A gives an additional degree of freedom in fitting the model to observations. We demonstrate that the proposed model predicts superlinear tumor growth, consistent with experimental results shown by Pérez-García *et al*. (2020). Scenario and contributions of our analysis are as follows:

- We elaborate and launch stochastic simulations for scenarios of cancer evolution with weakly advantageous mutations based on the Gillespie algorithm, for supporting and verifying further results of deterministic modelling.
- We formulate a deterministic model of tumor evolution as a system of differential balance equations for changes of expected numbers of cells with divisions and deaths, and for changes of expected numbers of occurring mutations.
- In this model of tumor growth solitary mutation wave propagates in cancer cells population. We obtain analytical relations concerning the propagation of the mutation wave (dynamics of mutation wave) in the growing population of cancer cells, in terms of the mean and variance of the number of mutations. In the previous literature, models of the dynamics of mutation of fitness waves were derived under the assumption of constant population size.
- We analyse the model of quasi-stationary mutation wave (mutation wave with variance approximately constant over time). Using the deterministic model augmented with the simple cutoff condition for number of cells (Tsimring *et al*., 1996; Sharp, 1982), we establish a deterministic numerical procedure for relating the variance of the quasi-stationary mutation wave with the population size.
- For the model of quasi-stationary mutation wave, we derive analytical relations for the growth rate of the cancer cells population. We verify the obtained deterministic, analytical results by stochastic simulations.
- We demonstrate that, for a reasonable selection of parameters, the tumor growth rate versus tumor size/volume increases superlinearly with an exponent parameter within the range consistent with the findings presented in reference (Pérez-García *et al*., 2020).

In our study, the force driving the growth of cancer cells population is the process occurring at the molecular level, of the emergence of somatic mutations during cellular replication and their propagation in cellular evolution. The scenario under consideration is more fundamental, and its mathematical modeling is less complex than the mathematical models of cancer growth at the level of cellular processes proposed in the referenced previous papers (Pérez-García *et al*., 2020; Azimzade *et al*., 2021; Bosque *et al*., 2023). Our models require only a few parameters, intensities of cellular births and deaths, probabilities of occurrences of weakly advantageous mutations and their fitness. Their approximate values can be found or estimated on the basis of the literature (e.g., Mc Farland *et al*, 2013; 2014). Our mathematical model explains the rate of growth of both solid tumors and blood cancers, while previously proposed models rather refer only to solid tumors. In the development of tumors and their understanding at the mesoscopic level there are many aspects such as spatial distribution, interactions with surrounding tissues, dynamics of angiogenesis, which are biologically very important, but their mathematical modeling is complicated.

2. Evolution scenario for the cancer cells

We study the evolution scenario of the cancer cells population with events of deaths, births and weakly advantageous mutations. These events are represented graphically in Fig. 1. Cell deaths and births are inhomogeneous Poisson processes with rates depending on the state of the model (defined by population size and the number of mutations in cancer cells). Random events of mutations are occurring during cell births. Cell death rate depends on the cancer cell population size, on the population capacity parameter and on the exponent parameter. Birth rates of cells depend on the number of (somatic, weakly advantageous) mutations in their DNA.

2.1. Notations for processes and events. In relation to the events shown in Fig. 1 we use the following notation.

$N(t)$ denotes population size, i.e., the expected number of cells in the analyzed cancer population and by N_C, we denote the population capacity parameter. We often drop t (time) writing $N(t) = N$, for conciseness.

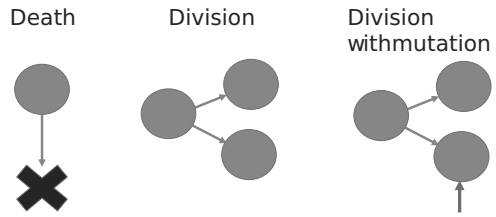

Fig. 1. Graphical representation of possible events in the analyzed scenario of cancer cells populations evolution.

The intensity of death processes is assumed to depend on the population size $N(t)$ and population capacity parameter N_C by a power function with exponent denoted by A (see (1)).

By l we denote the number of weakly advantageous passenger mutations in a cancer cell, $n_l(t) = n_l$ stands for the size (expected number of cells) of the subpopulation of cancer cells population, of cells harbouring l weakly advantageous passenger mutations. We also call the sub-population n_l-type or class with l mutations. By f we denote the value of the positive selection coefficient. The probability of acquiring a mutation in a cell division is denoted by p_f.

All variables and parameters presented above are listed in Table 1.

2.1.1. Death process. Intensity of the cellular death Poisson processes $\mu_D(N)$ depends only on the total number of cells N and on the population capacity parameter N_C, by the relation

$$\mu_D(N) = \left(\frac{N}{N_C}\right)^A. \tag{1}$$

The above relation between $\mu_D(N)$ and N is assumed as a power function with an exponent A. If the exponent is equal to one, $A = 1$, the model of the death intensity becomes the same as that used in the literature (McFarland *et al.*, 2013; 2014). Here, by allowing $A \neq 1$ we introduce one more degree of freedom in modelling. This additional degree of freedom has consequences to the rate of growth of cancer cells population with weakly advantageous mutations and allows us to fit our model to recently published experimental results on rates of growth of tumours (Pérez-García *et al.*, 2020).

2.1.2. Birth process. Birth rate of cells of type l, denoted by $\mu_B(l, f)$, is assumed to be described by the following function

$$\mu_B(l, f) = (1 + f)^l \simeq e^{lf}, \tag{2}$$

where approximation $e^f \simeq (1+f)$ is used. Accumulation of weakly advantageous mutations, according to the above function, increases the intensity of the birth process. Based on the assumption of the weak effect of mutations, we can linearize the birth rate function (2) for approximating values of $\mu_B(l, f)$

$$\begin{aligned} \mu_B(l, f) &\cong \mu_B(\chi_f, f)(1 + f(l - \chi_f)), \\ \mu_B(l-1, l) &\cong \mu_B(\chi_f, f)(1 + f(l - 1 - \chi_f)). \end{aligned} \tag{3}$$

The above linearization is around the mean value of the number of mutations in a cell χ_f, defined in the subsequent text in (6).

2.1.3. Mutation process. Mutations occur during cell divisions, with probability p_f, which leads to the intensity of mutations given by

$$p_f \mu_B(l, f), \tag{4}$$

where $\mu_B(l, f)$ is birth process intensity given by (2).

2.1.4. Values of parameters. Values of parameters of selection and mutation processes in the model are chosen by referring to the literature (McFarland *et al.*, 2013). The value of the negative selection coefficient of weakly deleterious passenger mutations was taken by these authors to be in the range $10^{-4} - 10^{-1}$. We take these values as a reference, and we assume a positive selection coefficient, f, of the order $10^{-4} - 10^{-3}$. Probability of mutations, p_f are taken to be of the order of $10^{-3} - 10^{-2}$. In the work of McFarland *et al.* (2013) similar values of probability of passenger mutations are obtained by multiplying mutation intensity per cell division event per nucleotide by the estimated number of target sites equal to be of the order of 10^6. The population size of cancer cells in our computations is assumed to be in the range from 10^3 to 10^6.

2.1.5. Units of time scale. In our model, the temporal progression is continuous and corresponds to the actual time elapsed during tumour evolution. It is scaled by the intensities of the birth-and-death process. The unit of time is assumed equal to the expected waiting time for the birth event in a "wild type" cell, with no mutations ($l = 0$). With values of parameters applied in our models one unit of time is considered to fall within the range of one day to one week.

3. Stochastic simulation model of evolution of cancer cells

The elaborated stochastic simulations algorithm for the evolution scenario described in the previous section is described below. We use Gillespie stochastic simulation method (Gillespie, 1976) to draw random times of

Table 1. Variables and parameters in deterministic and stochastic models and their explanations.

Symbol	Explanation	Units
$N(t)$	Cancer cells population size	Counts
N_C	Population capacity parameter	Counts
l	Number of weakly advantageous mutation in cancer cell	Counts
$n_l(t)$	Size of the subpopulation of cells with l mutations	Counts
f	Value of positive selection coefficient	Dimensionless
p_f	Probability of acquiring mutation in cell division	Dimensionless
A	Exponent of the power function describing cell death intensity	Dimensionless

events of cells deaths, divisions and mutations, based on intensities (1), (2) and probabilities (4). In our implementation of the Gillespie algorithm, the state of the process is N-dimensional vector, where N is the number of cells (population size), each element corresponds to one cell and its entry is determined by the number l of mutations harboured by the cell. Initially, the state vector contains entries equal to 0 since the initial mutation number is zero for all cells. The initial value of N is set to $N = N_C$.

In each simulation cycle/loop, time instants corresponding to potentially occurring events of deaths and births are randomly drawn from exponential distribution and scaled by intensities (1) and (2), following from population size and numbers of mutations in each cell. For each cell birth, a possible mutation event is generated randomly as a Bernoulli trial with probability p_f. To increase efficiency, we use the *tau-leap* version of the Gillespie algorithm (Marchetti *et al.*, 2017). The parameter of the simulation algorithm τ should be much smaller than the unit of time. Based on simulation experiments, we consider the range $0.005 \leq \tau \leq 0.05$ as a reasonable choice.

Values of randomly generated times of potential deaths and births and results of Bernoulli trials are then used to obtain binary vectors of events (*pdt*-death event, *pdv*-division event, and *pdm*-mutation event), which allow for appropriate updating of the state vector.

The whole simulation process is combined from multiple simulation loops where each loop increases simulation time by τ. Simulation terminates when the condition of the simulation time or population size is encountered.

4. Deterministic model of evolution of the population of cancer cells

Deterministic modelling involves formulating systems of differential equations describing the fitness effects of advantageous mutations as well as related laws behind cellular deaths and replications. On the basis of relations (1)–(2) we formulate a deterministic model of the evolution as the set of deterministic equations of balances of expected streams of dividing/dying cells and occurring passenger mutations. The set (system) of equations of balances of cells/mutations flows has the following form:

$$\frac{\mathrm{d}}{\mathrm{d}t}n_l = p_f\mu_B(l-1,f)n_{l-1} + (1-p_f)\mu_B(l,f)n_l - \mu_D(N)n_l. \quad (5)$$

The right-hand side has three components of the rate of change of a number of cells of type l. The first component is the rate of increase of the number of cells of type l due to cells of type $l-1$ acquiring mutation during their replications, the second component gives the rate of increase due to replications of cells of type l (division without mutation), finally, the third one is the rate of decrease due to cell deaths. The range of indices l is $l = 0, 1, 2 \ldots$.

4.1. Evolution of the population size. We can derive a differential equation governing the evolution of the population size—the total number of cells N equal to the sum of the numbers of cells over all cell types. We have $N = \sum_l n_l$ and we define mean χ_f and variance σ_f^2 of numbers of advantageous mutations

$$\chi_f(t) = \chi_f = \sum_l l\nu_l, \quad (6)$$

$$\sigma_f^2 = \sum_l (l-\chi_f)^2\nu_l, \quad (7)$$

where ν_l are frequencies of cells of type l:

$$\nu_l(t) = \frac{n_l(t)}{N(t)}. \quad (8)$$

Summing both sides of equations (5) over the range of values of l and using linear approximations (3) and relation (1) we get

$$\frac{\mathrm{d}}{\mathrm{d}t}N = \left[\mu_B(\chi_f,f) - \left(\frac{N}{N_C}\right)^A\right]N. \quad (9)$$

The above differential equation describes the dynamics of the size of the total cell population $N(t)$. Rewriting (9) as

$$\frac{1}{N}\frac{\mathrm{d}}{\mathrm{d}t}N = \left[\mu_B(\chi_f, f) - \left(\frac{N}{N_C}\right)^A\right] \tag{10}$$

and noting that N is large, one can notice that (5) with (10) can be considered as a two-time scale system (Kuehn, 2015). In the fast time scale we assume $\mu_B(\chi_f, f) \simeq const$, so starting from any initial condition the population size $N(t)$ tends to the fast time limit $N = N_C\mu_B(\chi_f, f)^{\frac{1}{A}}$. Slow time scale dynamics is given by the solution to (5) restricted to the manifold

$$N(t) = N_C\left[\mu_B(\chi_f(t), f)\right]^{\frac{1}{A}}. \tag{11}$$

4.2. Mutation wave. We describe mutation wave traveling in cancer cells population by deriving the dynamics of the change of the mean number of mutations $\chi_f(t)$. In order to derive equations describing the change of mean numbers of mutations over time we start by considering frequencies of cell types. We first differentiate both sides of (8) to obtain

$$\frac{\mathrm{d}}{\mathrm{d}t}\nu_l = -\frac{1}{N^2}\frac{\mathrm{d}N}{\mathrm{d}t}n_l + \frac{1}{N}\frac{dn_l}{\mathrm{d}t}. \tag{12}$$

By substituting (9) and (5) in the above equation, we get the set of differential equations describing the dynamics of $\nu_l(t)$,

$$\begin{aligned}\frac{\mathrm{d}}{\mathrm{d}t}\nu_l = \mu_B(\chi_f, f)[&p_f(1 + f(l - 1 - \chi_f))\nu_{l-1} \\ &- p_f(1 + f(l - \chi_l))\nu_l + f(l - \chi_f)\nu_l].\end{aligned} \tag{13}$$

Using the above, we derive a differential equation describing the time change of $\chi_f(t)$. We use equations for the dynamics of frequencies of cell types; see Eqn. (13). Multiplying both sides of (13) by l and summing up over the range of index l we obtain

$$\sum_l l(\frac{\mathrm{d}}{\mathrm{d}t}\nu_l) = \frac{\mathrm{d}}{\mathrm{d}t}(\chi_f) = \mu_B(\chi_f, f)(p_f + f\sigma_f^2). \tag{14}$$

4.3. Quasi-stationary profile of mutation waves in finite-size population. Equation (14) is used here for modeling propagation of the mutation wave. However, its efficient application requires elaborating a method for computing/estimating values of variance σ_f^2. Balancing forces, which influence values of σ_f^2, need accounting for the effects of the finite size of the cancer cell population and quantization of sub-populations (cell classes) n_l. The differential balance equations (5) are formulated in real numbers arithmetic, so they contain streams of cells and mutations generated in sub-populations n_l of fractional sizes (of sizes smaller than 1). In real cellular populations and in stochastic simulations sub-populations n_l generate cells and mutations when their size is bigger than 1. So here we use a simple (heuristic) modification of the deterministic model (5), which involves introducing the assumption that cell divisions in the cell class n_l can happen only if $n_l \geq 1$. Introducing the function $h(n)$ defined as

$$h(n) = \begin{cases} n & \text{if} \quad n \geq 1, \\ 0 & \text{if} \quad n < 1, \end{cases} \tag{15}$$

we formulate modified deterministic balance equations, as follows:

$$\begin{aligned}\frac{\mathrm{d}}{\mathrm{d}t}n_l = &\, p_f\mu_B(l - 1, f)h(n_{l-1}) \\ &+ (1 - p_f)\mu_B(l, f)h(n_l) - \mu_D(N)n_l.\end{aligned} \tag{16}$$

The condition for the size of cell classes analogous to (15) was already used in modeling evolution of fitness of RNA viruses in populations with constant size, where it was named cutoff condition (Tsimring *et al.*, 1996; Sharp, 1982). It is intuitively explained by the same argument as we are giving here and additionally supported by experimental and simulation results. Here we use the cutoff modification for the model with a growing population size. Analogously to the previous literature we observe that the deterministic model with cutoff condition (16) gives reasonably good consistency with stochastic simulations.

Comparison of numerical solutions of two models, differential system of differential equations (5) and modified differential equations with cutoff condition (16) is given in Fig. 2, for the parameters $A = 1$, $f = 0.0005$, $p_f = 0.025$, $N_C = 10\ 000$. Time plots corresponding to solutions (5) are drawn as dashed lines, while those representing (16) are drawn as solid lines. Initial conditions for both models are defined by initial population size $N(0) = N_C$ and the initial number of mutations in all cells $l = 0$. Numerical solutions are computed by the fourth-order Runge–Kutta algorithm. Qualitatively, both solutions are analogous, both predict the propagation of a mutation wave towards accumulating an increasing number of weakly advantageous passenger mutations by cancer cells and the increase of the population size $N(t)$. However, quantitatively the two scenarios of propagation differ significantly. The mutation wave computed based on (5) propagates faster. When represented by means and variances it is also broader (has larger variance) than that corresponding to (16). When comparing time plots of variances of mutation numbers, $\sigma_f^2(t)$ (right panel, middle plot), we see that the values of $\sigma_f^2(t)$ computed based on cutoff modified equations (16) (solid line) are approximately constant (precisely, they increase very slowly), while values of $\sigma_f^2(t)$ computed on the basis of differential equations (5) (dashed line) show a significant increase in time.

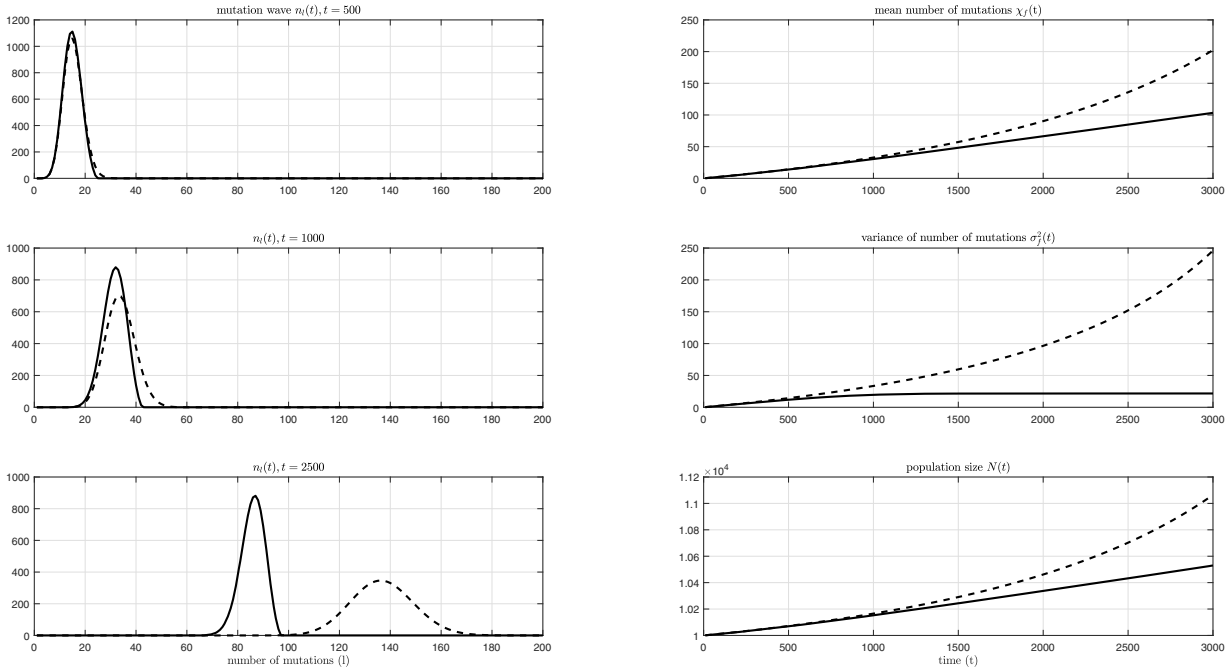

Fig. 2. Comparison of solutions of deterministic differential equations model (5), with the solution to model (16) with cutoff modification (15), for modelling evolution with weakly advantageous mutations, for the parameter set $A = 1$, $f = 0.0005$, $p_f = 0.025$, $N_C = 10\,000$. Left panels present plots of mutation waves at three time instants $t = 500$, $t = 1\,000$ and $t = 2\,500$. The right panels show time plots of mean numbers of mutations, $\chi_f(t)$ (upper plots), the variance of mutation numbers, $\sigma_f^2(t)$ (middle plots) and number of cells in the cancer population $N(t)$ (lower plots). For all plots, dashed lines show time plots computed by using numerical integration of the system of differential equations without (5) while analogous solid lines represent solutions to modified equations (16).

Additionally it can be seen that solutions to modified differential equations (16) are consistent with the results of stochastic simulations. This can be demonstrated by comparison analogous to that presented in Fig. 2. Deterministic modelling is based on differential equations with cutoff modification. Stochastic simulations are based on the Gillespie algorithm described in the previous subsection. The set of parameters assumed in computations is the same as that in Fig. 2: $A = 1$, $f = 0.0005$, $p_f = 0.025$, $N_C = 10\,000$. Here we assume a longer time range, from $t = 0$ to $t = 10\,000$. In Fig. 3 we show time plots corresponding to differential equations with cutoff modification (16) solved numerically by using the Runge–Kutta method, versus analogous time plots obtained by using stochastic simulations with the Gillespie algorithm. The deterministic differential equation model and Gillespie simulation algorithm were started with the initial condition given by initial population size $N(0) = N_C$ and the initial number of mutations in all cells $l = 0$.

In the plots of time change of $\sigma_f^2(t)$ corresponding to solutions of systems of cutoff modified equations (16) shown in Fig. 2 and Fig. 3 we observe quasi-stationarity of $\sigma_f^2(N)$. Variances of mutation numbers $\sigma_f^2(t)$ corresponding to propagating mutation waves are changing slowly in time. It is also the property of mutation waves seen stochastically in simulations in Fig. 3 (when variances of numbers of mutations are averaged over time).

Referring to the slow time relation (11) we accept the hypothesis that σ_f^2 is a slowly changing function of the population size N. Here we present the slow change of $\sigma_f^2(N)$ in quantitative terms. In Fig. 4 we show plots of functions $\sigma_f^2(N)$ for different values of positive selection coefficient ($f = 0.0005$, $f = 0.001$, $f = 0.0015$) and for different values of exponent parameter ($A = 0.1$, $A = 0.3$, $A = 0.5$, $A = 1$). Plots in Fig. 4 were obtained by multiple runs of a numerical algorithm for solving cutoff modified equations (16), with different values of N_C. It is seen from Fig. 4 that, while values of N change in the range of 3 orders of magnitude (from 10^3 to 10^6) the corresponding values of σ_f^2 span less than one order of magnitude (from 10 to 50). Plots corresponding to different values of A are drawn with different colours. Fig. 4, apart from showing slow growth $\sigma_f^2(N)$ as a function of N also demonstrates that changing the value of the exponent A makes almost no change in the plots of

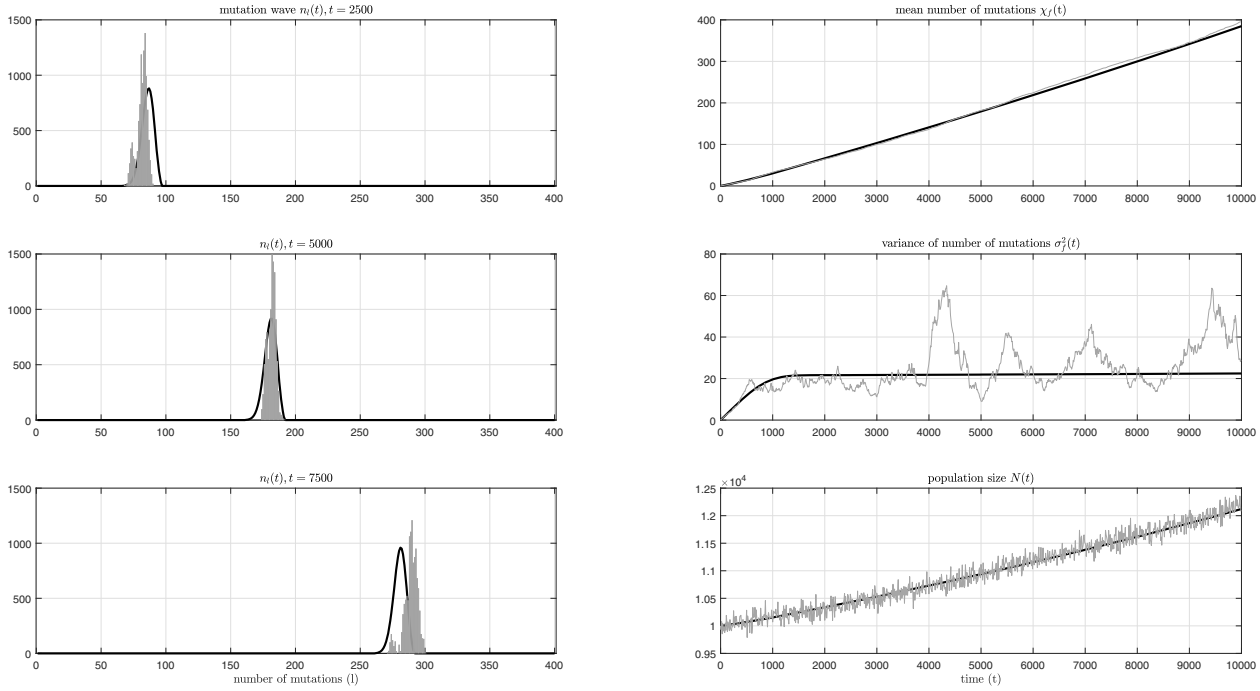

Fig. 3. Comparison of deterministic (with cutoff modification) versus stochastic modelling for evolution with weakly advantageous mutations, for the parameter set $A = 1$, $f = 0.0005$, $p_f = 0.025$, $N_C = 10\,000$. The left panels present plots of mutation waves at three time instants $t = 2\,500$, $t = 5\,000$ and $t = 7\,500$. The right panels show time plots of mean numbers of mutations, $\chi_f(t)$ (upper plots), the variance of mutation numbers, $\sigma_f^2(t)$ (middle plots), and the number of cells in the cancer population $N(t)$ (lower plots). For all plots, black, bold lines show time plots computed by using numerical integration of the system of differential equations with cutoff modification (16). Gray plots present the results of stochastic simulations obtained by using the Gillespie algorithm.

$\sigma_f^2(N)$.

Based on the above, in the model considered in the next subsection (for deriving the power law of the population size growth), we use an approximation

$$\sigma_f^2(N) = \sigma_f^2 \cong const. \tag{17}$$

4.4. Power law in the evolution of the population size. Evolution of the size of cancer cells population in the slow time with weakly advantageous mutations (11) is determined by the time change of mean numbers of mutations in cancer cells, $\chi_f(t)$, whose dynamics is described by differential equations (14). The equation for the velocity of the mutation wave (14), can be used to derive a model of the evolution of the population size in the slow time in the form of differential equations. Through this subsection, we accept the hypothesis on the slow change of variance; see Eqn. (17).

To derive a differential equation for the slow time evolution of the population size, we differentiate with respect to time both sides of (11), and we use (14). This leads to

$$\frac{\mathrm{d}}{\mathrm{d}t}N(t) = \frac{1}{A}N_C\left[\mu_B(\chi_f, f)\right]^{(1+\frac{1}{A})}(fp_f + f^2\sigma_f^2). \tag{18}$$

The above equation, by using (11), can be transformed to the differential equation with $N(t)$ as a state variable:

$$\frac{\mathrm{d}}{\mathrm{d}t}N(t) = \frac{1}{AN_C^A}N^{(1+A)}(fp_f + f^2\sigma_f^2). \tag{19}$$

By computing logarithms of both sides of the above equation, we have the relation

$$log_{10}(\frac{\mathrm{d}}{\mathrm{d}t}N(t)) = (1+A)log_{10}(N(t)) + \log_{10}\left(\frac{fp_f + f^2\sigma_f^2}{AN_C^A}\right), \tag{20}$$

which represents the power law in the population size growth. Logarithms of population size $\log_{10}(N(t))$ and the growth rate $\log_{10}(\frac{\mathrm{d}}{\mathrm{d}t}N(t))$ are dependent linearly with the coefficient $1+A$. Analytical solution to the differential equation (19) as

$$N(t) = \frac{N_C}{\left[1 - t(fp_f + f^2\sigma_f^2)\right]^{\frac{1}{A}}} \tag{21}$$

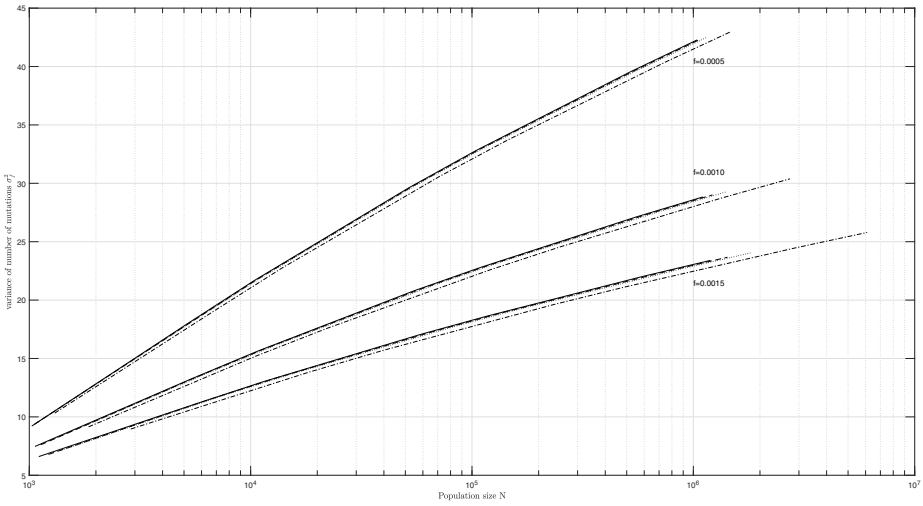

Fig. 4. Plots of functions $\sigma_f^2(N)$ for different values of the positive selection coefficient ($f = 0.0005$, $f = 0.001$, $f = 0.0015$) and for different values of the exponent parameter ($A = 0.1$, $A = 0.3$, $A = 0.5$, $A = 1$). Plots corresponding to different values of A are drawn with different line styles: $A = 0.1$ with a dash-dotted line, $A = 0.3$ with a dotted line, $A = 0.5$ with a dashed line, and $A = 1.0$ with a solid line.

exhibits a finite escape time,

$$t = \frac{1}{fp_f + f^2\sigma_f^2}. \tag{22}$$

We show a comparison of results of modelling the growth of the population size $N(t)$, by using a deterministic analytical solution (21) versus stochastic Gillespie algorithm, for parameters $f = 0.0005$, $p_f = 0.025$, $N_C = 10000$ and different values of exponent parameter A ($A = 0.1$, $A = 0.3$, $A = 0.5$ and $A = 1.0$) in cell death intensity relation (1). In Fig. 5(a) we present time plots $N(t)$, while in Fig. 5(b) we show plots of $\log_{10}(\frac{\mathrm{d}N}{\mathrm{d}t})$ versus $\log_{10}(N(t))$. Black bold curves in Figs. 5(a) and 5(b) are computed by using analytical solution (21) with approximation (17), where the variance is assumed to equal for all plots, $\sigma_f^2 = 25$ (this value was set on the basis of plots shown in Fig. 4 corresponding to $f = 0.0005$). Logarithmic plots in Fig. 5(b) demonstrate that for the range of change of population size $N(t)$ of the order of magnitude 1–2, the pattern of growth is well approximated by the power law (20).

5. Growth rates of tumours measured by positron emission tomography (PET)

Growth plots shown in Figs. 5(a) and 5(b) prove that growth rates of the size of the cancer cells population can be approximated by power functions with exponent $1 + A$. In Fig. 5a, we have shown approximations of cancer cells population growth for $1 + A$ ranging from 1.1 to 2 and for population size increased by more than one order of magnitude. Growth patterns presented in Fig. 5(b), showing growth intensity versus population size in logarithmic scales, can replicate analogous, experimentally measured plots published by Pérez-García *et al*. (2020). In Fig. 1(a–h) from that work, values of exponents of power laws range from 1.182 to 1.386 and ranges of sizes of tumour cell populations cover 1–2 orders of magnitude. These values can be easily reproduced by assigning suitable values to the exponent parameter A in our modelling, confirmed by the Gillespie simulation algorithm.

6. Discussion and conclusions

Mathematical and simulation models of asexual evolution with mutation waves travelling/propagating in populations of cells/organisms have already been extensively studied. The majority of approaches concern constant size population, the Wright–Fisher or Moran models of evolution. The classical result (Haigh, 1978), concerning mutations bringing deleterious effects, is a Poisson-like quasi-stationary distribution of sizes of mutation classes (mutation front) in a constant-size population. In the deterministic model, the position of the mutation front is fixed, while stochastic effects cause advance of the mutation wave/front by the mechanism called Muller's ratchet (Muller, 1932). Later studies developed many quantitative aspects concerning estimating the speed of advance of the mutation front (Gordo and Charlesworth, 2000). Several studies analyze, with the assumption of constant population size, evolution with advantageous mutations (Desai and Fisher, 2007; Uecker and Hermisson, 2011; Neher, 2013). In the context

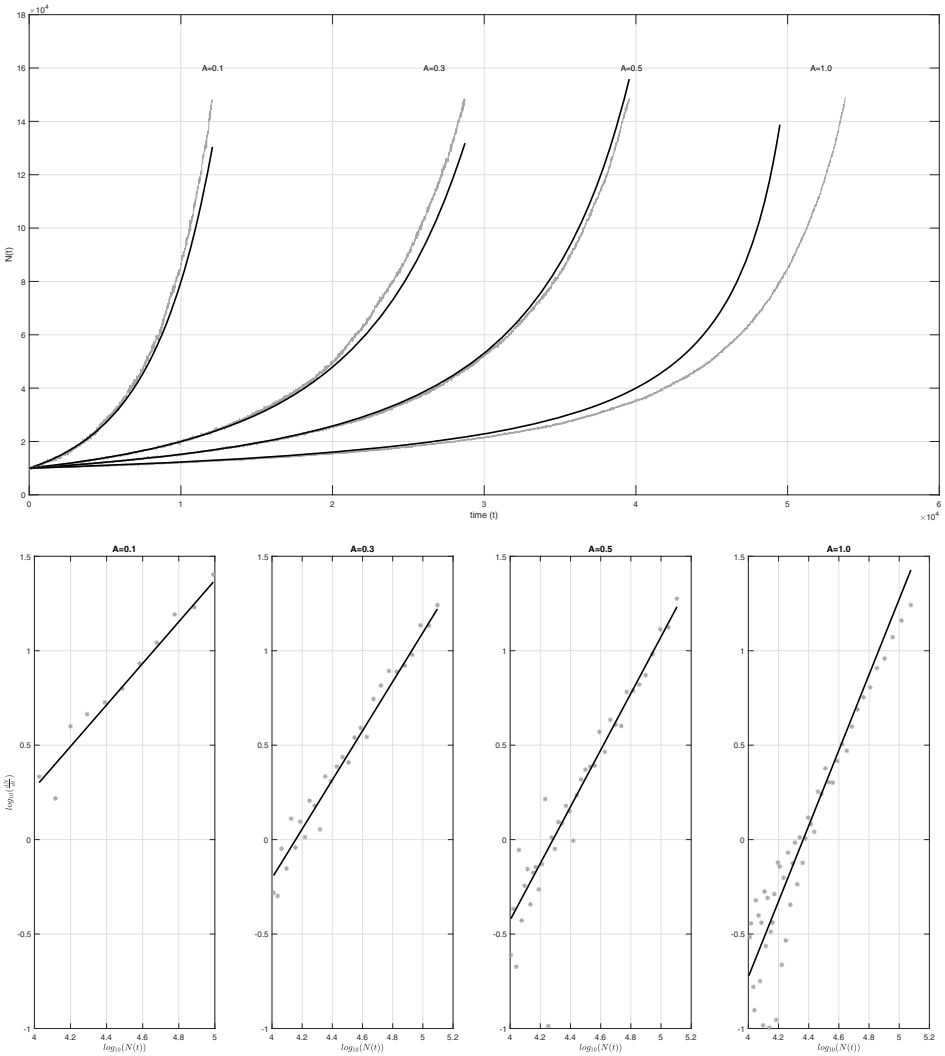

Fig. 5. Comparisons of growth patterns of cancer cells population size $N(t)$, for evolution with weakly advantageous mutations, for parameters $f = 0.0005$, $p_f = 0.025$, $N_C = 10000$ and different values of exponent parameter A in cell death intensity relation (1). Values of A used in computations/simulations are $A = 0.1$, $A = 0.3$, $A = 0.5$ and $A = 1.0$. Time plots $N(t)$: time plots $N(t)$ computed by using the analytical relation (21) are drawn with bold black lines, time plots of $N(t)$ obtained by using stochastic modelling (Gillespie algorithm) are drawn as grey curves (a)—top. Plots of $log_{10}(\frac{dN}{dt})$ versus $log_{10}(N(t))$: plots obtained by using (20) are drawn as black, bold lines. Growth patterns of $N(t)$ obtained on the basis of stochastic simulations (grey plots in Fig. 5(a)) are represented by grey asterisks. The coordinates of each asterisk are computed as base 10 logarithms of averaged values of $N(t)$ (horizontal coordinate) and $\frac{dN}{dt}$ (vertical coordinate). Averaging over bins of the size 1 000 in the time scale is done for the purpose of reducing the large variation of $\frac{dN}{dt}$ in stochastic simulations (b)—bottom.

of advantageous mutations, often the interest of the researchers is in estimating the probability of fixation or the time to fixation (Desai and Fisher, 2007; Uecker and Hermisson, 2011). Neher (2013) proposed the mathematical model of the process of fast adaptation driven by advantageous mutations, in the form of a coalescent with multiple mergers. Rouzine *et al*. (2003) as well as Desai and Fisher (2007) models of evolution with constant population size and two types of mutations, mildly deleterious and mildly advantageous, are studied. Evolution is described in terms of waves/fronts of fitness, which summarize counteracting effects of two possible types of mutations. The studies by Rouzine *et al*. (2003) as well as Desai and Fisher (2007) use different modelling techniques, however, they come to quite consistent results. Waves and mean population fitness, which appear in their scenarios follow from the combined effect of deleterious and advantageous mutations and depend on mutation intensities and values of selection/fitness coefficients and the population size.

In the works of Park *et al*. (2010) as well as Park and Krug (2013), several methodologies for estimating the speed of the wave of advantageous mutations in constant-size populations are presented and discussed. In the research by McFarland *et al.* (2013; 2014) (already mentioned in Introduction) a model of evolution with rare, strongly advantageous driver mutations and counteracting mildly deleterious passenger mutations is proposed for cancer cell populations. The size of the cancer cells population is not assumed constant but follows from the influence of the environment with a given capacity parameter and from the effects of occurring mutations. Mildly (weakly) deleterious passenger mutations lead to a slow, gradual decrease in the fitness of cancer cells, while driver mutations cause positive selective sweeps and define the clonal structure of the cancer cell population.

Here we have elaborated and studied models of the evolution of the cancer cells population inspired by McFarland *et al* (2013; 2014). Their model of propagating mutations in differs from Fisher–Wright or Moran type models in two important aspects. First, the size of the cancer cells population is not assumed to be constant, as in Fisher–Wright and Moran models, but follows from the influence of the environment with a given capacity parameter and from the effects of occurring mutations. Second, the time lapse is continuous, scaled by the intensity of the birth process and therefore can be related to the real time lapse in tumor progression. In the Fisher–Wright and Moran models time scales are either measured in generations or are given by discrete sequences of deaths and births occurring simultaneously. The two above differences make principles of modeling given by Mc Farland *et al.* (2013; 2014) a suitable tool for studying scenarios of tumor growth and growth rates. In our study we have simplified and modified the models of Mc Farland *et al.* (2013; 2014) by assuming that mutations can only have weakly advantageous effect on the fitness of cancer cells and that cell deaths process has the intensity given by the power function (1), with exponent parameter A. The function describing cell death intensity (1) is different (more general) than that of Mc Farland *et al.* (2013; 2014), where $A = 1$ was assumed. Allowing different values of A gives an additional degree of freedom in fitting the model to observations.

We have formulated a deterministic model of cancer cell evolution and verified this model by stochastic simulations, based on the Gillespie algorithm. Our deterministic model was defined as a system of differential equations for balances of numbers of cells and numbers of mutations with a cutoff condition, $n_l < 1$. Solutions to cutoff modified equations (16) show reasonably good agreement with the results of stochastic simulations, as demonstrated in Fig. 3. Mutation wave is quasi-stationary, it shows a very slow increase of variance in time. The variance of the mutation wave (Fig. 4) depends on the value of the parameter f (decreases with the increase of the fitness parameter f) and shows very small changes versus changing the exponent parameter A.

On the basis of deterministic balance equations, we derive a model for the propagation of the mutation wave in the population of cancer cells. The model of propagation (14) is analogous to relations derived in several papers (Rouzine *et al*., 2003; Neher, 2013), called Fisher's equation (Neher, 2013), or breeder's equation (Heywood, 2005). However, in contrast to these studies, the differential equation (14) describes the process evolving in the real time scale of tumor growth. It has the scaling factor $\mu_B(\chi_f, f)$, which reflects the phenomenon that cells with a greater number of mutations proliferate at a faster rate.

The observation of variance $\sigma_f^2(N)$ changing slowly as a function of N (see Fig. 4) motivates us to use constant approximation $\sigma_f^2 = const$ (17). With this assumption, we study the dynamics of the slow change of the population size. We use the model of the dynamics of the mean number of mutations (14) to write a differential equation for the slow time change of the population size (20), and then we obtain an analytical solution (21). The approximation $\sigma_f^2 = const$ works well for changes of $N(t)$ within orders of magnitude 1–2, as illustrated in Figs. 5(a) and 5(b). However, using the constant approximation $\sigma_f^2 = const$ has limitations. When changes in the population size N are larger than approximately two orders of magnitude, the resulting increase of σ_f^2 would change the dynamics. The growth would accelerate.

In the supplement to the work of McFarland *et al.* (2013) the authors present a simplified model of evolution, in the form of a single differential equation, for tumor growth driven by counteracting driver and passenger mutations. The model has only one compartment and its construction relies on the assumptions that only fixed mutations can influence the proliferation of cells and that fixation of mutations occurs instantly. The evolution of the size of the cancer cells population follows from an imbalance between the effects of occurring passenger and driver mutations. Depending on which force is stronger, the population either expands or goes to extinction. The fate of the cancer cells population depends on the initial population size, above some critical value expansion occurs, while the population with an initial size below the critical value would extinct. This model predicts the growth scenario with the growth rate exponent equal to 2. Our approach is more detailed, bases on stratification of cells into compartments corresponding to numbers of harboured somatic mutations and leads to analytical estimates consistent with stochastic simulations with the growth rate exponent $1 + A$.

The formula for growth rate (20) has an interesting form. The growth rate does not depend on parameter

f (positive selection coefficient) and p_f (probability of mutation), but only on the exponent parameter A of the death process intensity (1). It may seem counter-intuitive, but an increase in A actually results in an increase of the exponent of the tumor growth rate function.

Concluding, we have elaborated modeling tools for the growth of the cancer cell population driven by weakly advantageous mutations. The deterministic model shows agreement with the results of stochastic simulations and allows us to estimate the width and velocity of the mutation wave, and to predict the pattern of growth of the population size. With the elaborated model we are able to predict the pattern of cancer cells population growth with the growth rate proportional to N^{1+A}; see Eqn. (19). This pattern of growth, when choosing values of A in the range from 0.182 to 0.386, is consistent with the experimental results of Pérez-García *et al*. (2020).

7. Data and software availability

Our implementation of the Gillespie simulation algorithm described in Section 3 is available at `https://pypi.org/project/seEvo1D/`.

Acknowledgment

This publication was supported by the Department of Computer Graphics, Vision, and Digital Systems, Silesian University of Technology (Gliwice, Poland) under a statutory research project (Rau6, 2025) and co-financed by the European Union through the European Social Fund (grant POWR.03.02.00-00-I029 (Mateusz Kania)).

References

Azimzade, Y., Saberi, A.A. and Gatenby, R.A. (2021). Superlinear growth reveals the allee effect in tumors, *Physical Review E* **103**(4): 042405.

Bosque, J.J., Calvo, G.F., Molina-García, D., Pérez-Beteta, J., Vicente, A.M.G. and Pérez-García, V.M. (2023). Metabolic activity grows in human cancers pushed by phenotypic variability, *Iscience* **26**(3): 106118.

Boyko, A.R., Williamson, S.H., Indap, A.R., Degenhardt, J.D., Hernandez, R.D., Lohmueller, K.E., Adams, M.D., Schmidt, S., Sninsky, J.J., Sunyaev, S.R., White, T.J., Nielsen, R., Clark, A.G. and Bustamante, C.D. (2008). Assessing the evolutionary impact of amino acid mutations in the human genome, *PLoS Genetics* **4**(5): e1000083.

Bozic, I., Antal, T., Ohtsuki, H., Carter, H., Kim, D., Chen, S., Karchin, R., Kinzler, K.W., Vogelstein, B. and Nowak, M.A. (2010). Accumulation of driver and passenger mutations during tumor progression, *Proceedings of the National Academy of Sciences of the United States of America* **107**(43): 18545–18550.

Brú, A., Albertos, S., Subiza, J.L., García-Asenjo, J.L. and Brú, I. (2003). The universal dynamics of tumor growth, *Biophysical Journal* **85**(5): 2948–2961.

Cerami, E., Gao, J., Dogrusoz, U., Gross, B.E., Sumer, S.O., Aksoy, B.A., Jacobsen, A., Byrne, C.J., Heuer, M.L., Larsson, E., Antipin, Y., Reva, B., Goldberg, A.P., Sander, C. and Schultz, N. (2012). The CBIO cancer genomics portal: An open platform for exploring multidimensional cancer genomics data, *Cancer Discovery* **2**(5): 401–404.

Davydov, E.V., Goode, D.L., Sirota, M., Cooper, G.M., Sidow, A. and Batzoglou, S. (2010). Identifying a high fraction of the human genome to be under selective constraint using GERP++, *PLoS Computional Biology* **6**(12): e1001025.

Desai, M.M. and Fisher, D.S. (2007). Beneficial mutation selection balance and the effect of linkage on positive selection, *Genetics* **176**(3): 1759–1798.

Fu, Y., Liu, Z., Lou, S., Bedford, J., Mu, X.J., Yip, K.Y., Khurana, E. and Gerstein, M. (2014). FunSeq2: A framework for prioritizing noncoding regulatory variants in cancer, *Genome Biology* **15**(10): 480.

Gillespie, D.T. (1976). A general method for numerically simulating the stochastic time evolution of coupled chemical reactions, *Journal of Computational Physics* **22**(4): 403–434.

Gordo, I. and Charlesworth, B. (2000). The degeneration of asexual haploid populations and the speed of Muller's Ratchet, *Genetics* **154**(3): 1379–1387.

Greaves, M. and Maley, C.C. (2012). Clonal evolution in cancer, *Nature* **481**(7381): 306–313.

Haigh, J. (1978). The accumulation of deleterious genes in a population—Muller's ratchet, *Theoretical Population Biology* **14**(2): 251–267.

Heywood, J.S. (2005). An exact form of the breeder's equation for the evolution of a quantitative trait under natural selection, *Evolution* **59**(11): 2287–2298.

ICGC/TCGA PCWG Consortium (2020). Pan-cancer analysis of whole genomes, *Nature* **578**(7793): 82–93.

Jiao, W., Atwal, G., Polak, P., Karlic, R., Cuppen, E., Danyi, A., de Ridder, J., van Herpen, C., Lolkema, M.P., Steeghs, N., Getz, G., Morris, Q.D. and Stein, L.D. (2020). A deep learning system accurately classifies primary and metastatic cancers using passenger mutation patterns, *Nature Communications* **11**(1): 728.

Kuehn, C. (2015). *Multiple Time Scale Dynamics*, Springer, Berlin.

Kühleitner, M., Brunner, N., Nowak, W.-G., Renner-Martin, K. and Scheicher, K. (2019). Best fitting tumor growth models of the von Bertalanffy–Pütter type, *BMC Cancer* **19**(683): 1–11.

Kumar, S., Warrell, J., Li, S., McGillivray, P.D., Meyerson, W., Salichos, L., Harmanci, A., Martinez-Fundichely, A., Chan, C.W.Y., Nielsen, M.M., Lochovsky, L., Zhang, Y., Li, X., Lou, S., Pedersen, J.S., Herrmann, C., Getz, G., Khurana, E. and Gerstein, M.B. (2020). Passenger mutations in more than 2,500 cancer genomes: Overall molecular functional impact and consequences, *Cell* **180**(5): 915–927.e16.

Laird, A.K. (1964). Dynamics of tumour growth, *British Journal of Cancer* **18**(3): 490.

Marchetti, L., Priami, C. and Thanh, V.H. (2017). *Simulation Algorithms for Computational Systems Biology*, 1st Ed., Springer International Publishing, Cham.

McDonald, T.O., Chakrabarti, S. and Michor, F. (2018). Currently available bulk sequencing data do not necessarily support a model of neutral tumor evolution, *Nature Genetics* **50**(12): 1620–1623.

McFarland, C.D., Korolev, K.S., Kryukov, G.V., Sunyaev, S.R. and Mirny, L.A. (2013). Impact of deleterious passenger mutations on cancer progression, *Proceedings of the National Academy of Sciences of the United States of America* **110**(8): 2910–2915.

McFarland, C.D., Mirny, L.A. and Korolev, K.S. (2014). Tug-of-war between driver and passenger mutations in cancer and other adaptive processes, *Proceedings of the National Academy of Sciences of the United States of America* **111**(42): 15138–15143.

Muller, H.J. (1932). Some genetic aspects of sex, *The American Naturalist* **66**(703): 118–138.

Neher, R.A. (2013). Genetic draft, selective interference, and population genetics of rapid adaptation, *Annual Review of Ecology, Evolution, and Systematics* **44**(1): 195–215.

Noorbakhsh, J. and Chuang, J.H. (2017). Uncertainties in tumor allele frequencies limit power to infer evolutionary pressures, *Nature Genetics* **49**(9): 1288–1289.

Park, S.-C. and Krug, J. (2013). Rate of adaptation in sexuals and asexuals: A solvable model of the Fisher–Muller effect, *Genetics* **195**(3): 941–955.

Park, S.-C., Simon, D. and Krug, J. (2010). The speed of evolution in large asexual populations, *Journal of Statistical Physics* **138**: 381–410.

Pérez-García, V. M., Calvo, G.F., Bosque, J.J., León-Triana, O., Jiménez, J., Perez-Beteta, J., Belmonte-Beitia, J., Valiente, M., Zhu, L., García-Gómez, P., Sánchez-Gómez, P., Hernández-San Miguel, E., Hortigüela, R., Azimzade, Y., Molina-García, D., Martinez, Á., Rojas, Á. A., de Mendivil, A.O., Vallette, F., Schucht, P., Murek, M., Pérez-Cano, M., Albillo, D., Honguero Martínez, A.F., Jiménez Londoño, G.A., Arana, E. and García Vicente, A.M. (2020). Universal scaling laws rule explosive growth in human cancers, *Nature Physics* **16**(12): 1232–1237.

Rouzine, I.M., Wakeley, J. and Coffin, J.M. (2003). The solitary wave of asexual evolution, *Proceedings of the National Academy of Sciences of the United States of America* **100**(2): 587–592.

Salvadores, M., Mas-Ponte, D. and Supek, F. (2019). Passenger mutations accurately classify human tumors, *PLoS Computational Biology* **15**(4): e1006953.

Sharp, R.P. (1982). Landscape evolution (a review), *Proceedings of the National Academy of Sciences of the United States of America* **79**(14): 4477–4486.

Talkington, A. and Durrett, R. (2015). Estimating tumor growth rates in vivo, *Bulletin of Mathematical Biology* **77**: 1934–1954.

Tsimring, L.S., Levine, H. and Kessler, D.A. (1996). RNA virus evolution via a fitness-space model, *Physical Review Letters* **76**(23): 4440.

Tung, H.-R. and Durrett, R. (2021). Signatures of neutral evolution in exponentially growing tumors: A theoretical perspective, *PLoS Computational Biology* **17**(2): e1008701.

Uecker, H. and Hermisson, J. (2011). On the fixation process of a beneficial mutation in a variable environment, *Genetics* **188**(4): 915–930.

Vaghi, C., Rodallec, A., Fanciullino, R., Ciccolini, J., Mochel, J.P., Mastri, M., Poignard, C., Ebos, J.M. and Benzekry, S. (2020). Population modeling of tumor growth curves and the reduced gompertz model improve prediction of the age of experimental tumors, *PLoS Computational Biology* **16**(2): e1007178.

Vogelstein, B. and Kinzler, K.W. (2015). The path to cancer—Three strikes and you're out, *New England Journal of Medicine* **373**(20): 1895–1898.

Wang, H.-Y., Chen, Y., Tong, D., Ling, S., Hu, Z., Tao, Y., Lu, X. and Wu, C.-I. (2018). Is the evolution in tumors Darwinian or non-Darwinian?, *National Science Review* **5**(1): 15–17.

West, J. and Newton, P.K. (2019). Cellular interactions constrain tumor growth, *Proceedings of the National Academy of Sciences of the United States of America* **116**(6): 1918–1923.

Wilks, C., Cline, M. S., Weiler, E., Diehkans, M., Craft, B., Martin, C., Murphy, D., Pierce, H., Black, J., Nelson, D., Litzinger, B., Hatton, T., Maltbie, L., Ainsworth, M., Allen, P., Rosewood, L., Mitchell, E., Smith, B., Warner, J., Groboske, J., Telc, H., Wilson, D., Sanford, B., Schmidt, H., Haussler, D. and Maltbie, D. (2014). The cancer genomics hub (CGHub): Overcoming cancer through the power of torrential data, *Database* **2014**, bau093, DOI: 10.1093/database/bau093.

Williams, M.J., Werner, B., Barnes, C.P., Graham, T.A. and Sottoriva, A. (2016). Identification of neutral tumor evolution across cancer types, *Nature Genetics* **48**(3): 238–244.

WSI (2022). Catalogue of somatic mutations in cancer (cosmic), Wellcome Sanger Institute, Hinxton, `http://www.sanger.ac.uk/genetics/CGP/cosmic/`.

Andrzej Polański received his PhD and DSc degrees in automatic control from the Faculty of Automatic Control, Electronics, and Computer Science, Silesian University of Technology, Gliwice, Poland, in 1991 and 2000, respectively. In 2009 he was granted the professorial title by the President of Poland. He is the author and a co-author of more than 100 publications. His scientific interests include bioinformatics, populations genetics, biomathematical modeling, modeling and control of dynamical systems.

Mateusz Kania received his PhD in technical computer science and telecommunications from the Silesian University of Technology in Gliwice, Poland, in 2023. He is currently an assistant lecturer in the Department of Applied Computer Science at the same university and also works as a data scientist in the industry. His research focuses on both

supervised and unsupervised machine learning and the analysis of complex datasets. Outside of work, he is passionate about Argentine tango and stays active through various sports.

Jarosław Gil received his PhD degree in computer science in 2025. His research interests include bioinformatics, cheminformatics, and numerical modeling. He is interested in the topics of modeling and simulation of complex systems, including the clonal evolution of cellular populations using the Gillespie algorithm, explosion dynamics, and shockwave propagation.

Wojciech Łabaj received his PhD degree in biomedical engineering in 2020. He is employed as an assistant professor at the Silesian University of Technology, Gliwice, Poland. His research interests focus on data analysis and algorithm development for biotechnology and biomedical engineering applications. He works at the intersection of computer science, engineering, and technology, with particular emphasis on the analysis of DNA and RNA sequencing data. He is involved in developing innovative computational methods to support biomedical research and improve healthcare solutions.

Ewa Lach received her PhD degree in computer science in 2006. She is an assistant professor at the Silesian University of Technology, Gliwice, Poland. Her research interests include the application of artificial intelligence and mobile technologies in cognitive and motor function evaluation, particularly in aging populations. She is interested in the use of sensors, virtual and augmented reality, and depth cameras to personalize user experience and adapt game-based and diagnostic systems. She is the author and a co-author of more than 40 publications. Her work combines elements of biomedical engineering, cognitive science, human-computer interaction, and AI-based data analysis.

Agnieszka Szczęsna received her PhD and DSc degrees in computer science in 2007 and 2019, respectively. She is an associate professor at the Silesian University of Technology, Gliwice, Poland, and the head of the Department of Computer Graphics, Vision and Digital Systems at the Faculty of Automatic Control, Electronics and Computer Science there. She teaches in the topics area of computer graphics and rendering. Her scientific interests focus on the following issues: analysis of biomedical data, acquisition, analysis and synthesis of motion data, computer graphics and issues related to computer games, including the use of artificial intelligence. She participates in R&D projects in cooperation with companies.

Received: 18 November 2024
Accepted: 6 May 2025